

AJTE99-6153

A PROGRESS REPORT ON THE NIST CONVECTIVE HEAT FLUX CALIBRATION FACILITY

DAVID G. HOLMBERG
CAROLE A. WOMELDORF

Fire Science Division
Building and Fire Research Laboratory
National Institute of Standards and Technology
Gaithersburg, MD 20899

Keywords: calibration, convection, heat flux, standards, uncertainty

ABSTRACT

The National Institute of Standards and Technology has developed a convective heat flux calibration facility to allow evaluation of heat flux sensors. This facility is a small wind tunnel that produces a two-dimensional laminar boundary layer across a heated iso-thermal copper plate, figure A-1. This facility has been developed to allow convection calibration of heat flux sensors to complement heat flux sensor calibrations presently conducted using standard radiation methods, recognizing that many sensors are used in mixed radiation and convection environments. By extending calibration capabilities

to include a primarily convective environment, direct comparisons of sensors in controlled convective and radiative environments are possible.

This report describes the first-generation heated plate design and performance. The reference heat flux on the plate is found from the electrical power input to a guarded region of the plate to the side of the sensor in the spanwise uniform flow. Tests have demonstrated a repeatability on the reference heat flux of $\pm 1.5\%$. A detailed uncertainty analysis of the reference heat flux value is presented showing lateral conduction to surrounding regions of the plate to be the greatest source of uncertainty with plate surface emissivity the only other significant source. The calculated relative expanded uncertainty (95 % level of confidence) on the measured reference heat flux value is $\pm 4.6\%$. The average reference heat flux from these tests agrees with numerical predictions within 2 %.

An independent measure of the reference heat flux has been employed to demonstrate absolute accuracy of the facility. Tests using a conduction calibration agree within 1 % with the plate reference. This 1 % difference gives increased confidence in the absolute accuracy of the convection facility and compares favorably with the calculated 4.6 % uncertainty.

Development of a second generation heated plate continues with the goal of reducing uncertainty on the reference heat flux. Testing of sensors in the current heated plate is on-going.

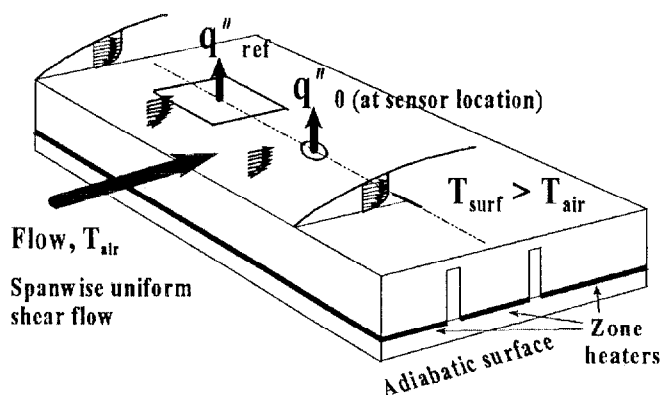


Figure A-1: Heated plate below laminar boundary layer with reference region to determine undisturbed heat flux at sensor.

INTRODUCTION

Heat flux sensors are typically calibrated in a known radiation flux, but used in a combined radiation and convection environment. The heat transfer community has recognized that this dichotomy contributes to relative measurement uncertainties no better than $\pm 10\%$ [1]. Collective realization of the absence of standards for calibration and the lack of understanding of the issues involved in heat transfer measurement led to a workshop at NIST in 1995 to discuss calibration and measurement issues and to delineate the current NIST calibration project. This workshop is described in references [1,2].

The primary goal of the NIST project is to develop three heat flux calibration facilities as standards for calibration to a desired relative uncertainty of $\pm 2\%$. The first facility is the low-speed convection wind tunnel discussed herein, with flux levels less than 10 kW/m^2 . The second facility is a higher flux (100 kW/m^2) conduction facility [3], and the third an upgraded radiation facility [4]. For the first time, these facilities will allow a sensor to be calibrated at NIST in each of the three heat flux modes independently.

BACKGROUND

Heat flux is the movement of thermal energy through a surface, with units of power per area. This flow is controlled by sensor structure, sensor material properties and radiation characteristics, as well as fluid motion and properties. It is fundamentally difficult to measure this energy flow without disturbing it—each sensor has structure with varying material properties that can disturb the flow of energy through the sensor, and surface properties that differ from the surrounding surface. Accurate measurement of heat flux requires understanding the errors produced by any given sensor which may vary depending on the nature of the incident energy.

The internal structure and surface properties of a sensor can significantly change the flux through the sensor relative to the desired undisturbed flux through the surrounding surface.

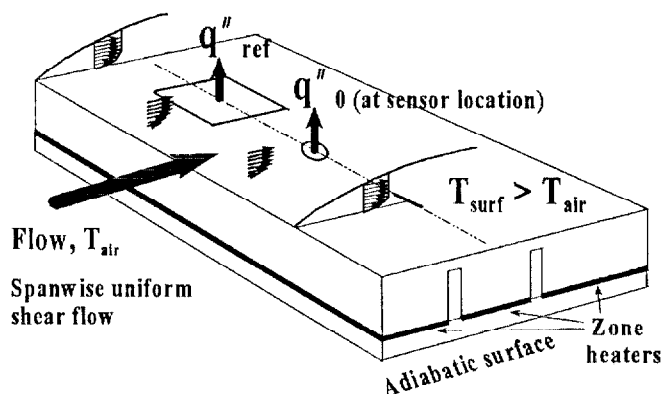


Figure 1: Heated plate below laminar boundary layer with reference region to determine undisturbed heat flux at sensor.

Heat transfer from a sensor attached to a heated surface is generally by conduction to the sensor surface and from the surface by convection to the air and radiation to the surroundings. If the sensor structure includes lower thermal conductivity elements (such as adhesive or resistance layers) these can significantly alter the surface temperature profile relative to the surrounding surface and thus change the local heat flux. Convection from the sensor surface will be disrupted if there is any change in surface roughness or discontinuity of the surface profile. Radiation exchange may not match that of the surrounding surface because any given sensor absorbs, reflects, and transmits according to its own surface properties.

The need for convection calibration can be seen when considering these effects. A radiation calibration is typically a short-duration measurement with the sensor at the surrounding plate temperature. The calibration is relatively insensitive to sensor temperature and mounting because the radiation source temperature is much higher than the sensor temperature and because the conduction path through the sensor may not be as important for short times. However, in convection both sensor temperature and conduction path become sensitive calibration parameters due to the relatively low flow to sensor temperature difference and steady state nature of the calibration.

MEASUREMENT OF HEAT FLUX AND THE NIST CONVECTION FACILITY

Measurement of heat flux is performed using a variety of methods which can be classified in three categories: (1) a temperature difference measured across a material of known thickness and thermal conductivity, (2) a temperature difference measured over time with a known thermal capacitance, and (3) a direct measure of the energy transfer made at steady conditions. References [5-7] review these methods and some of their different applications.

NIST's convective heat flux facility uses a steady state electrical heater output (category three above) as a reference. Because the facility operates at steady state, it is not configured to provide a reference heat flux value for transient (category two) temperature measurements. Instead, the facility is designed to test category one sensors that measure heat flux from a temperature difference.

The present NIST facility is best suited for mounting the insert plug-type sensors, and can also handle some of the smaller flat sensors. The NIST facility will be used to research heat transfer issues such as the sensitivity of different sensor types to convection versus radiation, the effects of sensor mounting, and the influence of surface coatings.

FACILITY DESIGN

The convection facility is a small open-loop wind tunnel with flow conditioning designed to produce a repeatable two-dimensional laminar flow across a heat flux sensor mounted in a heated isothermal plate. The maximum heat flux with the present configuration is approximately 6 kW/m^2 (at $\Delta T_{flow} = 100 \text{ K}$). Measurements from a sensor are calibrated against the

power required to heat a guarded reference section located alongside the sensor in the plate, Fig. 1. Following are details of the wind tunnel construction, test section components, and instrumentation.

The convection facility is depicted in Fig. 2. After passing through upstream flow conditioning elements, the air enters a two-dimensional contraction nozzle which reduces the flow cross section from 300 mm x 300 mm to 10 mm x 300 mm. This 30:1 contraction ratio was chosen to minimize inlet turbulence intensity and provide a “top-hat” velocity profile with a very thin boundary layer entering the test section. Design of the nozzle and exit velocity measurements are presented in [8]. Flow visualization has demonstrated a spanwise uniform two-dimensional slot flow entering the test section over the reference section and sensor areas of the plate.

Heated plate

The present design of the test section includes a heated, isothermal, copper plate beneath a laminar shear flow of room temperature air. A bottom view of the plate is shown in Figure 3. Grooves divide the plate into partially thermally isolated regions, for a total of 6 regions (labeled A-F) heated independently by six DC power supplies. The paired regions: A, B, and C, are joined in series. By independently heating the six regions, temperature variation can be controlled and conductive perimeter losses can be compensated. Polyimide/metal foil resistance heaters (0.1 mm thick) are attached with a pressure sensitive adhesive layer to the bottom of each region. Below the heaters is a layer of insulation and beneath this, a guard heater to null bottom conductive losses. Additional insulation and a support plate are beneath this, with the entire sandwich held in place by a clamp pressing the plate upward against the precision-located sidewalls to align the plate leading edge with the nozzle exit.

The heat flux sensor mounts in a copper cylinder (sensor housing) that seats against the lip seen in the center hole of the plate in Fig. 3. This allows the sensor surface to be set flush

with the upper surface of the plate at a known distance from the inlet of the test section.

Reference region

The reference value for the undisturbed heat flux at the sensor location is determined from the power input to the region of the plate labeled REF in Fig. 3. Power is found by measuring voltage across the REF region heater along with the voltage drop across a precision resistor to measure heater current. Power to surrounding regions and the lower guard heater are adjusted to null conduction in and out of the reference region so that the power to the REF region exits only from the upper surface.

The plate surface temperature is monitored with 32 fine gage (36 AWG) type-T (Copper-Constantan) thermocouples. Ice-point calibration of these thermocouples has allowed uncertainties of 0.05 K for absolute temperature measurements. Two differential thermocouple pairs on each side of the REF region monitor the temperature difference across the bridge spanning the air gap. Tests have demonstrated 0.01 K accuracy for these differential measurements (0.01 K uncertainty at a 95 % level of confidence, based on statistical analysis of data samples). The thermocouple, differential thermocouple, heat flux sensor, and power signals are collected with a PC-based data acquisition system. A feedback control algorithm automatically adjusts power to the heaters in order to minimize temperature differences and thereby null lateral conduction.

UNCERTAINTY ANALYSIS FOR HEATED PLATE

The reference heat flux value is based on knowing the energy transferred from the reference area to the air flow above and by radiation to the surroundings. The reference area must be guarded to prevent conductive heat transfer from the reference heater to and from surrounding regions in the plate. Conduction out the bottom must also be minimized and any other losses accounted for. Uncertainties arise from system

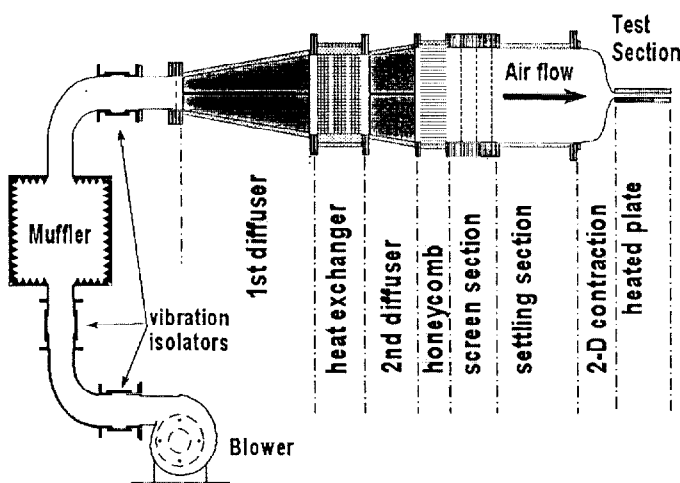


Figure 2: Schematic of wind tunnel flow conditioning.

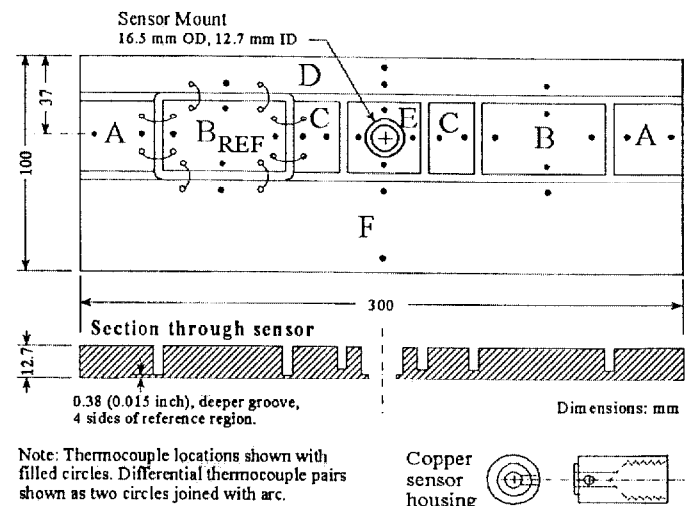


Figure 3: Bottom view of heated plate showing sensor location, separate regions of plate, and sensor holder.

limitations on controlling parasitic conduction to surrounding regions within the plate, and knowledge of surface radiation properties. Relating the reference heat flux to the flux at the sensor introduces additional uncertainties. In this section, uncertainties of the reference heat flux value will be discussed, first looking at conduction uncertainties and then at the radiation uncertainties. Finally, an analysis is given for additional uncertainties in relating the heat flux from a test gage mounted in the hot plate to the reference value.

It will be shown that the primary uncertainty is due to lateral conduction to or from the reference area to surrounding regions. This uncertainty is absolute, determined by the accuracy to which the temperature between and within regions can be controlled and measured. This lateral conduction flux is independent of the convective flux to the flow. Therefore, the percentage of this lateral flux relative to the convective flux decreases with increasing plate to air temperature difference. Testing has been performed at differences up to 100 K.

I. Reference Heat Flux Uncertainties

A. Conduction within plate

The reference area is 32.0 mm x 54.0 mm, plus a surrounding gap width of 3.2 mm. It is assumed for this analysis that the reference heated area includes half the gap width. The deviation from this assumption has been calculated theoretically and found to be insignificant. Therefore, the total heated area including half the gap width is $2.01 \times 10^{-3} \text{ m}^2$. Uncertainty estimates will be made for a plate to flow temperature difference $\Delta T_{\text{flow}} = 40 \text{ K}$. The convective energy transferred from the reference section to the flow, based on the convective numerical model described later is $q_{\text{conv}} = 4.90 \text{ W}$, or $q''_{\text{conv}} = 2440 \text{ W/m}^2$.

1. Lateral conduction analysis. Lateral conduction is affected by several parameters, shown in Fig. 4. The copper surface bridges the air gap separating the reference area from surrounding heated regions. Lateral conduction across this metal bridge increases with plate thermal conductivity and bridge thickness, but decreases with gap width. The accuracy of the differential temperature measurement, 0.01 K stated earlier, is that between the two thermocouple beads. However, because of thermal gradients in the plate, the value measured is not necessarily the average difference across the bridge along the length of a reference area side. Taking the average of two differential thermocouples along each side helps to reduce this uncertainty. For this analysis, the uncertainty (estimated standard deviation based on system experience and modeling results to follow) on the temperature difference across the gap is taken as $\Delta T_{\text{gap}} = 0.025 \text{ K}$.

The conduction across the bridge around the reference section is

$$q_{\text{gap}} = kPd \frac{\Delta T_{\text{gap}}}{w};$$

$k = 400 \text{ W/mK}$; P is the perimeter, measured at the gap center (0.185 m); d is the bridge thickness (0.38 mm); and w is the

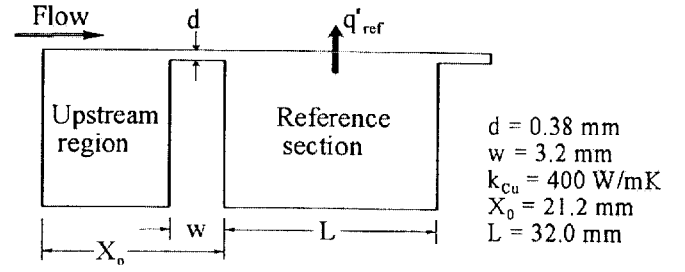


Figure 4: Side view of heated plate reference section and upstream region showing bridge across air gap and dimensions for first generation heated plate.

gap width (3.2 mm). The amount of energy transferred across the gap if there is an undetected 0.025 K temperature difference between the reference area and all surrounding regions (RSS of the error for each of the four sides) is $q_{\text{gap}} = 0.11 \text{ W}$. This amount of heat transfer cannot be reduced with the present plate because it is derived from the physical system and the accuracy of temperature measurement. Taking this as the uncertainty due to uncontrollable conductive heat transfer to surrounding regions, the current design (at $\Delta T_{\text{flow}} = 40 \text{ K}$) has a *lateral conduction uncertainty* (estimated standard deviation on lateral conduction) $= q_{\text{gap}}/q_{\text{conv}} = 2.2 \%$.

A conduction model of the thermal field in the plate and sensor has been developed to investigate issues related to improvement of the present plate design [9]. This model includes the convective flow as a boundary condition on the upper surface of the plate using the $x^{-1/2}$ theoretical isothermal plate heat transfer distribution.

Results from this model have clearly shown the presence of gradients in the plate primarily due to the conduction of energy required to heat the bridge between regions. An estimate of the magnitude of the thermal contours in the gap region for the present plate are shown in Fig. 5. At the ideal balanced condition, the surface of each region in the plate

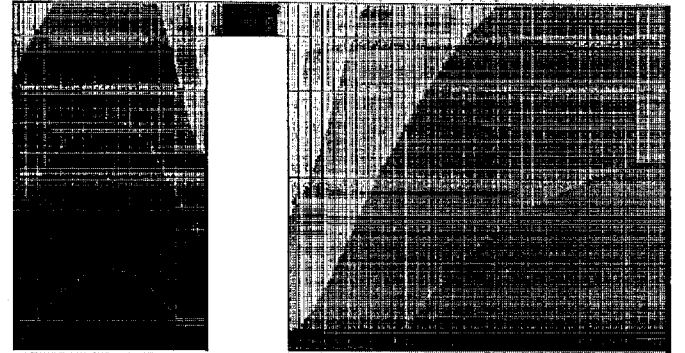


Figure 5: Temperature gradients in present plate, looking from side (as in Fig. 4) at the upper 2 mm of the plate, from the center of the upstream region D (left) to the center of the reference region (right) for $T_{\text{plate}} - T_{\text{air}} = 40 \text{ K}$. Not to scale. Contour gradients, $\Delta T = 0.01 \text{ K}$.

would be isothermal and all regions would be at the same temperature. In actuality, there are several hundredths of a degree Kelvin temperature variation along the surface near the bridge as well as within the bridge, as seen in Fig. 5. Experimentally, a temperature measurement is made with a small thermocouple bead near the surface of the plate inserted in a hole from the bottom side. Since the desired accuracy of temperature measurement across the bridge is of the same order as the temperature variation seen due to thermal gradients, it is clear that the choice of materials, bridge design, and placement of thermocouples are important issues in the redesign of the heated plate. These gradients support the 0.025 K uncertainty on the temperature difference estimated above.

In the air gap, lateral conduction and natural convection have been considered. Heat transfer by conduction through the air is less than 0.01 % of the reference convective flux. Because the air gap is close to isothermal, the Rayleigh number turns out to be more than 2 orders of magnitude less than the critical value above which natural convection would occur. Thus, the air is stationary with insignificant conduction.

2. Reference section bottom losses. Thermocouples embedded at two different vertical locations in the foam beneath the reference heater allow monitoring the temperature gradient across the foam and nulling it by adjusting power to the guard heater. A temperature uncertainty across the insulation of 1 K is assumed, based on experience, with a total heat transfer area approximately equal to the reference area. The foam has a thermal conductivity of $k_{\text{foam}} = 0.030 \pm 10\%$ W/mK and thickness of $h = 0.010$ m. Therefore the uncertainty in the bottom conductive loss is $q_{\text{cond, bottom}} = k_{\text{foam}} \cdot A \cdot \Delta T / h = 0.006$ W. This amount of energy, transferred across the foam insulation with a 1 K temperature difference, results in a *bottom conduction uncertainty* of $q_{\text{cond, bottom}} / q_{\text{conv}} = 0.1\%$.

3. Wire conduction losses. Both thermocouple leads and power leads to the heaters are paths for conduction away from the heated plate. The thermocouple leads are Teflon coated 36 awg wire, while the heater wires are stranded copper. These leads exit the reference area below the heaters, cross the gap to the neighboring regions, and then are routed along the bottom of the plate and out through the insulation to room air. The wires remain in a nearly isothermal environment for at least 100 mm. Accordingly, their impact can be estimated in a manner similar to the upper gap bridge. Neglecting conduction along the insulation, 4 thermocouple wires, 8 differential thermocouple wires, and two heater wires (19 strands each) have a net cross section of 1.2 mm^2 . Taking the conductivity of all the wires at $k_{\text{Cu}} = 400$ W/mK, and a conservative estimate of $\Delta T = 0.1$ K across the 3.2 mm gap, the q_{loss} will be 1.4×10^{-4} W, or less than 0.003% of q_{conv} .

4. Heat flux distribution. Knowledge of the heat flux as a function of distance streamwise along the plate is required to know the relationship between the sensor flux and the reference flux. The measured reference power is an average value over the heated area.

The heat flux distribution can be found both by numerical modeling and by reference to theoretical isothermal flat plate heat transfer which varies as $x^{-1/2}$ where x is the distance from the plate leading edge. Integration of this profile across the reference area produces an average heat flux proportional to the measured reference heat flux. The flux at the sensor, taken as a point measurement, equals the flux at the center of the reference area. Based on this distribution, the ratio of the heat flux at the center point to the average is $q''_{\text{sens}} / q''_{\text{ref}} = 0.969$. This agrees with the numerical solution to the conjugate conduction and convection heat transfer problem [8], and this correction is applied to the reference heat flux value.

B. Radiation from the plate

The present plate emissivity is uncertain because *in-situ* measurements were not performed and the polished surface has light oxidation (in the second generation plate, a non-oxidizing surface will be used). An estimate of the current surface emissivity is $\epsilon_{\text{ref}} = 0.10 \pm 0.05$. Taking the surroundings (test section top surface, nozzle, room walls, etc.) at room temperature, we can simplify the view factor to $F = 1.0$ and regard the surroundings as a hemispherical blackbody at room temperature (297 K). Then the radiation heat transfer from the reference area is $29.0 \pm 14.5 \text{ W/m}^2$, given T_{ref} equal to 337 K. This flux is 1.2 % of the convective flux at $\Delta T_{\text{flow}} = 40$ K, with 0.6 % relative uncertainty due to emissivity uncertainty.

The combined standard uncertainty on the reference heat flux for the present heated plate design operating at $\Delta T_{\text{flow}} = 40$ K, taken as the square root of the sum of the squares of the lateral conduction, bottom conduction, and radiation uncertainties discussed above is

$$u_c = \sqrt{u_{\text{lat cond}}^2 + u_{\text{bottom cond}}^2 + u_{\text{rad}}^2} = 2.3\%$$

Assuming that the measured reference heat flux values follow a normal distribution with a standard deviation of approximately 2.3 %, the actual true heat flux, including convective and radiative components, will be $q''_{\text{ref}} \pm 4.6\%$, where $U = 4.6\%$ is the expanded uncertainty and a coverage factor of $k = 2$ has been applied so that the unknown true value lies within the interval of $U = k \cdot u_c$ with a 95 % confidence level [10].

II. Sensor Heat Flux Uncertainties

A. Conduction within sensor housing

The present sensor housing is made of copper. The sensor has a sliding fit in the center hole, held by a set screw and using thermal grease to reduce contact resistance. The sensor housing itself is mounted in the plate with a sliding fit and thermal grease. The housing and sensor rely on heating by conduction from the surrounding plate, region E, and will generally be below the temperature of the surrounding plate. The sensor itself has internal structure that may limit conduction to its surface and further lower the temperature of the sensor body. Qualitative evaluation with liquid crystals showed that the center of one sensor was several degrees below the temperature of the surrounding region. A non-uniform temperature profile

in the sensor region can potentially change the thermal boundary layer profile. Computational results have shown that the boundary layer in the present test section recovers quickly relative to sensor dimensions and that the error in assuming an undisturbed heat transfer coefficient profile is small relative to other uncertainties [11].

B. Sensor radiation heat flux

The sensor analysis is very similar to that for the reference area, except that the emissivity of test sensors will vary and will typically be near unity. A typical sensor may have $\epsilon_{\text{sensor}} = 0.85$ with some manufacturer supplied uncertainty on this value. Assuming the sensor sees only room temperature black surroundings, the radiative flux from the sensor will be $q''_{\text{rad,sensor}} = 247 \text{ W/m}^2$ at $\Delta T_{\text{flow}} = 40 \text{ K}$, or 9.2 % of the total flux from the sensor. Uncertainty in ϵ_{sensor} will strongly affect $q''_{\text{rad,sensor}}$ which will in turn affect the uncertainty on q''_{total} . To control the total uncertainty due to this radiation component, the emissivity of the sensor surface must be supplied by the manufacturer. Heating of the test section upper surface would reduce the radiation component and is being planned for the second generation design.

REPEATABILITY TESTS

Two test series are reported. The first series examines the ability of a heater control algorithm to arrive at the same reference heat flux value given a randomized start condition and the same external boundary conditions. The second series examines sensitivity of the reference heat flux value to installation factors including sensor housing, heated plate and insulation, and test section structure.

For both test series, the plate to flow temperature difference was set to 40 K. Power to the plate heaters was shut off between tests and the plate allowed to cool. Tests were begun by allowing the heater control program to turn on the power and bring the plate temperatures to a balanced state. The “balanced” condition requires that the final plate to flow temperature difference equal the set temperature difference (within 1 K for these tests), and that the average differential temperature on each side of the reference region equals zero within some convergence criteria, set to 0.015 K for these tests. After balancing the plate temperatures, the system was usually left at this stable condition for several hours to monitor system drift. Reported reference heat flux values are normalized on the actual temperature difference.

These tests were performed using an improved test section support structure that differs from that reported in [8]. The new arrangement allows more accurate alignment of the plate leading edge and upstream thermal guard to the contracting nozzle exit so that the air flow is passed along a smooth surface into the test section. This is a critical issue due to the thin boundary layer, 0.5 mm thick, at the nozzle exit.

First test series: convergence repeatability

In the first test series, a total of 13 data points were collected over a period of 10 days. These data points are presented in Fig. 6 as a function of time. The test section was left assembled throughout the series. The power to the plate heaters was shut off for a short time (typically 20 min) between tests and a random array of power settings (within 20% of the final converged power levels) was sent to the plate heaters at the start of each test. The control algorithm then balanced the plate temperatures and saved data to file after the plate had “converged” as defined in the software. The average convergence time was approximately 6 hours.

After the first 10 data points were taken (in the course of a week) it appeared that there was a rise in the data to some more stable value after the first three or four data points. This would indicate a much longer system time constant in operation, perhaps due to very slow heating of the test section and tunnel and thermal expansion effects. To check this, the tunnel was allowed to cool for three days and then the final three data points taken. These appear to confirm the rise seen in the first three data points. The variation seen in points 4 through 10 may be more representative of the lateral conduction uncertainty with the current control algorithm, while the rise is likely an indicator of a real change in the reference flux due to system changes affecting the convective boundary layer, rather than reference heat flux measurement error.

Using all these data gives a sample mean of $q''_{\text{ref,avg}} = 2647 \text{ W/m}^2$ and sample standard deviation of $s = 17$. The tail area probability at the 0.025 level of the t distribution with 12 degrees of freedom is $t_{12,0.025} = 2.179$. This gives a 95 % level of confidence on the true mean of $q''_{\text{ref}} = q''_{\text{ref,avg}} \pm s \cdot t_{12,0.025} = 2647 \pm 38$ ($\pm 1.4 \%$). This value indicates the accuracy of the control algorithm and also stability of the facility over 10 days time with heating and cooling of the plate and support structure. If points 4 through 10 are isolated to remove the long

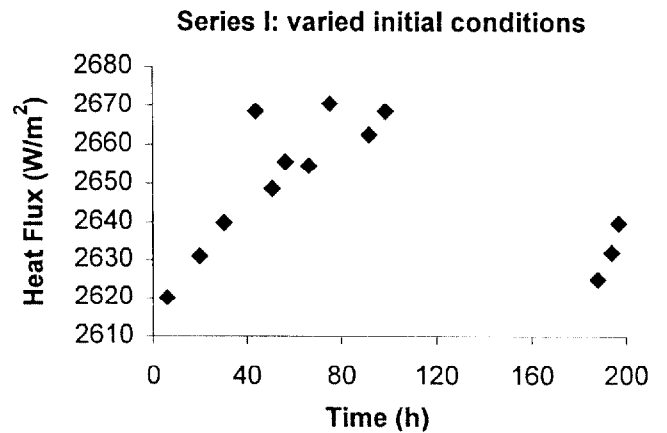


Figure 6: First series test data: converged reference heat flux result of successive measurements with varied initial heater power settings.

term transient, then the 95 % level of confidence on the true mean is $q''_{ref} = q''_{ref,avg} \pm s \cdot t_{6,0.025} = 2661 \pm 21$ (± 0.8 %). This value indicates repeatability assuming the facility has been in operation for several days. It is likely that this long time constant effect is mostly correctable and that this lower repeatability estimate is achievable. This $U = 0.8$ % measured (type A) expanded uncertainty of the reference heat flux value gives an indication of the actual lateral conduction uncertainty, but does not include radiation uncertainty. The following test series investigates the added uncertainty of installation variables.

Second test series: installation effects

For the second test series, the sensitivity of the reference heat flux to several installation variables: re-installation of the sensor, sensor housing, plate position, and test section side walls with upstream thermal guard, were investigated. These are not independent variables because the test section side walls cannot be removed without disturbing other parameters, and the plate cannot be removed without disturbing the sensor housing. For some tests, only the sensor housing was removed and replaced, or the heated plate was removed and replaced, and several times the entire test section was taken apart and re-assembled. Each test was begun using the same initial power. However, because the system was disturbed between each test, the control algorithm was run to bring the system to a balanced condition and then data were written to file.

The converged reference heat flux values are shown in Fig. 7 as a function of time. The mean heat transfer is significantly lower than test series I. After series I was completed, some previous damage to one corner of the test plate was found and repaired resulting in proper alignment of the plate for series II. Therefore, the difference in heat flux is real and due to aerodynamic changes, and the plate positioning for the second test series is in agreement with the

computational modeling performed. Figure 7 shows a rise in mean heat flux after the first three points similar to that seen in series I. This also corresponds to the disassembly of the test section side walls and upstream thermal guard after tests 3, 5, and 8. There appears to be some correlation with this action, but the reference heat flux appeared insensitive to all other factors. It was noticed that the thermal guard seemed to change position such that the alignment of the plate to thermal guard and guard to nozzle exit changed during the testing with correlation to the initial rise seen here. Misalignments of approximately 0.1 mm maximum were noted, apparently due to thermal expansion effects. This is a correctable effect and may also explain the rise seen in the first series.

Using these data gives a sample mean of $q''_{ref,avg} = 2331$ W/m^2 and sample standard deviation of $s = 15$. The 95 % level of confidence on the true mean is $q''_{ref} = q''_{ref,avg} \pm s \cdot t_{10,0.025} = 2331 \pm 34$ (± 1.5 %). This precision is in agreement with the series I results. It appears, as desired, that the converged reference heat flux value is insensitive to initial heater power settings, while the variation seen in both series is due primarily to the accuracy of the differential temperature measurement as well as the noted initial transient rise.

CONDUCTION CALIBRATION PLATE TESTS

To further substantiate the accuracy of the facility, a secondary reference has been employed. The conduction calibration plate is a water cooled aluminum plate with a mirror finish that sits above the heated plate separated by precision ball bearings (mounted in a rubber gasket) at its edges. Stagnant room air is the conducting gas with known thermal conductivity [12]. This provides a reference conduction heat flux based on a known temperature difference across an air gap with a known separation distance. The mirror finish minimizes radiation heat transfer, and the surface hemispherical spectral reflectance of the cold plate has been measured (the total hemispherical emissivity, integrating over the IR spectrum, is $\epsilon = 0.020$) so that radiation can be accurately accounted for. Radiation and conduction combined give a total flux that serves as a secondary absolute reference which can be compared to the measured system reference heat flux.

Uncertainty analysis of calibration plate heat flux

The reference flux of the conduction calibration plate will be called the predicted value, q''_{pred} . Sources of uncertainty in this value are listed in Table 1. All uncertainty estimates are type B: based on information other than statistical analysis of sampled data. Following Table 1: the estimate for the uncertainty on k_{air} (1 %) is given by the authors of the NIST Air Properties Database [12] as generally applicable to gas phase thermal conductivity measurements. A careful study of the effects of humidity on thermal conductivity, based on the work of Melling et. al. [13], showed that for typical mole fractions of water in room temperature air, humidity variation has only a small effect on thermal conductivity. The

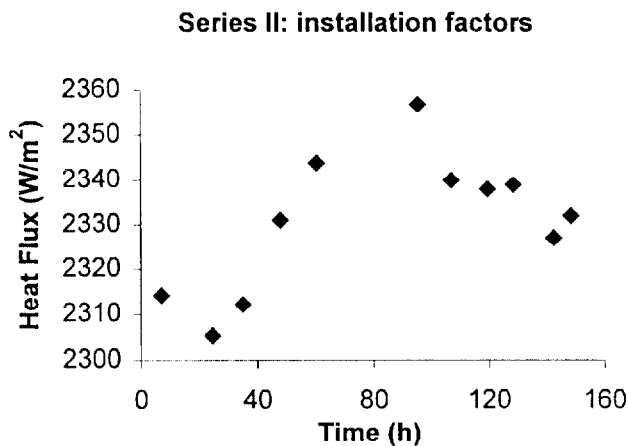


Figure 7: Second test series: converged reference heat flux result of successive runs with varied installation factors.

Table 1 Conduction calibration plate reference heat flux uncertainties.

Uncertainty name	relative standard uncertainty, u_i (%)	source for uncertainty estimate
k_{air} (thermal cond.)	1.0	ref [12]
humidity variation	0.1	analysis based on ref [13]
h_{gap} (plate sep. distance)	0.8	0.025mm / 3.18 mm
temperature difference	0.06	0.05 K / 80 K
$\epsilon_{\text{hotplate}}$	0.2	perturb $0.03 < \epsilon_{\text{hotplate}} < 1.0$
$\epsilon_{\text{coldplate}}$	0.15	perturb $0.015 < \epsilon_{\text{coldplate}} < 0.025$
infinite plate assumption	0.1	see explanation in text

uncertainty on the separation between the plates is due to plate flatness considerations. Temperature uncertainty refers to the uncertainty on the temperature difference between the two plates. The effect on the reference heat flux of the uncertainty of the emissivity values for the hot and cold plates was determined by perturbing their values in the q''_{pred} calculation. The infinite plate uncertainty is an estimate for this configuration of the uncertainty associated with assuming infinite parallel plate radiation exchange between finite plates.

Clearly, gas thermal conductivity and gap height are the largest sources of uncertainty, with a combined relative standard uncertainty of $u_c = 1.3$ %. Assuming the measured calibration plate reference heat flux values, q''_{pred} , follow a normal distribution, with a standard deviation of approximately 1.3 %, the actual true heat flux will be $q''_{\text{pred,avg}} \pm 2.6$ %, where $U = 2.6$ % is the expanded uncertainty and a coverage factor of $k = 2$ has been applied.

Calibration plate results

The results of 11 tests over a one week period are presented in Figure 8. Tests were performed at a nominal temperature difference of $T_{\text{hotplate}} - T_{\text{coldplate}} = 80$ K, with a separation distance of 3.18 mm. The system was disturbed between each test, requiring re-balancing of the power to the

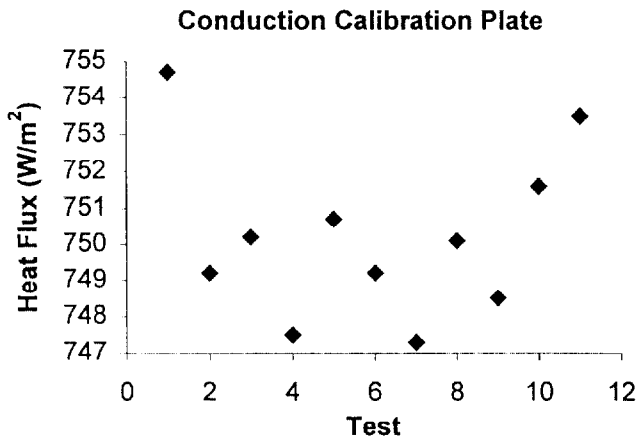


Figure 8: Normalized plate reference section heat flux measurements from conduction calibration plate tests.

heaters. Before each test the surface of the mirror was cleaned (outgassing of the gasket caused some organic condensate to collect near the cold plate edges), and the cold plate reset above the hot plate. Between several tests the sensor housing was removed and replaced.

The data presented in Fig. 8 is normalized by the predicted flux based on actual plate temperatures for each test.

$$q''_{\text{ref, norm}} = q''_{\text{ref}} \times \frac{q''_{\text{pred, avg}}}{q''_{\text{pred}}}$$

where the average predicted flux, $q''_{\text{pred, avg}} = 726.5$ W/m² ($U = 2.6$ %) is the independent calculated reference flux based on conduction. These data give a sample mean of $q''_{\text{ref, avg}} = 750.2$ W/m² and sample standard deviation of $s = 2.3$ W/m². The tail area probability at the 0.025 level of the t distribution with 10 degrees of freedom is $t_{10, 0.025} = 2.228$. This gives a 95 % level of confidence on the true mean of $q''_{\text{ref}} = q''_{\text{ref, avg}} \pm s \cdot t_{10, 0.025} = 750.2 \pm 5.2$ (± 0.7 %). These tests demonstrate the excellent repeatability of the heated plate reference section, better than found in the convection repeatability tests (0.7 % vs. 1.5 % uncertainty). The increased uncertainty in the presence of convection is due in part to added uncertainty associated with an aerodynamic boundary layer and non-uniform heat flux.

The most important result of these tests is demonstration of the heated plate reference section accuracy. In this case, the heated plate reference heat flux, $q''_{\text{ref, avg}} = 750.2$ W/m², is 3.3 % above the predicted “true” heat flux value for these tests, $q''_{\text{pred, avg}} = 726.5$ W/m² (itself with a relative expanded uncertainty of 2.6 %). This 3.3 % error says that at this flux level (730 W/m²) the lateral conduction losses at the heated plate “balanced” condition amount to 3.3 % of the total flux leaving the top of the heated plate, or 24 W/m². At the higher convective flux of 2400 W/m² (for $\Delta T_{\text{flow}} = 40$ K) this parasitic loss would be unchanged and can be expected to result in only a 1.0 % error. Therefore, the conduction calibration plate has established the absolute accuracy of the heated plate reference independent of other measures.

FUTURE WORK

Several projects are under way, including evaluation of different heat flux sensors with the present heated plate as well as construction of a second generation heated plate. Interaction with U.S. heat flux sensor manufacturers has led to the

acquisition of several common types of sensors that will be tested in the convection facility. Testing of these sensors will lead to better understanding of performance in convective versus radiative environments.

The second generation heated plate is being designed to reduce system uncertainty on the reference heat flux, and to allow multiple sensor locations and redundant references. The conduction code discussed earlier has been used to investigate different reference section designs. Uncertainty on lateral conduction is being reduced with a gap redesign and an increase in the number of independently heated plate regions. Sensor flux uncertainties will be reduced through more direct heating of the sensor and also through use of a heated test section upper surface to control radiation losses. The goal is to reduce the relative expanded uncertainty on the reference heat flux to below the 2 % level.

CONCLUSIONS

The NIST convective heat flux calibration facility has seen continued development to its present state as a fully operational facility allowing automated balancing of plate temperatures and measurements of reference heat flux with a repeatability of ± 1.5 %. An uncertainty analysis on the reference region heat flux value has shown lateral conduction to surrounding regions of the plate to be the greatest source of uncertainty with plate surface emissivity the only other significant source. The calculated relative expanded uncertainty (95 % confidence level) on the measured reference heat flux value is ± 4.6 %.

Accuracy of the measured reference heat flux value has been judged by comparison to theory, numerical modeling, and independent conduction calibration plate results. The repeatability test series II average heat flux of 2331 W/m^2 is 1.9 % below the numerical model prediction of 2376 W/m^2 corrected for radiation. This 1.9 % difference between measured and predicted values supports the accuracy of the facility and numerical code. Likewise, the conduction calibration plate results demonstrate that at a flux level of 2400 W/m^2 the measured reference heat flux is 1.0 % above the conduction calibration plate's independent reference flux. This 1.0 % difference gives increased confidence in the absolute accuracy of the convection facility and compares favorably with the calculated 4.6 % uncertainty.

Work continues on the second generation heated plate design and with test measurements in the current facility.

ACKNOWLEDGMENTS

The support of Prof. Alfonso Ortega (University of Arizona) and of Mr. Kenneth Steckler (NIST Building Fire Research Laboratory) on the wind tunnel design is greatly appreciated. The support of Dr. David Blackburn (NIST Electronics and Electrical Engineering Laboratory) and Dr. Ronald Davis (NIST Chemical Science and Technology Laboratory) with numerical modeling have contributed to this work. Mr. Robert Zarr's (NIST Building Fire Research Laboratory) thermal conductivity measurements are also

appreciated. The assistance of Dr. Daniel Friend (NIST Physical and Chemical Properties Division) with thermal conductivity issues is much appreciated. The help of Dr. Leonard Hanssen (NIST Physics Laboratory) with hemispherical reflectance measurements is greatly appreciated. Finally we acknowledge the support and guidance of Dr. William Grosshandler (NIST Building Fire Research Laboratory, Fire Science Division, Fire Sensing Group leader).

REFERENCES

- [1] Diller, T.E., "Heat Flux Calibration -- Progress Toward National Standards," Proceedings of the 41st International Instrumentation Symposium, Denver, CO, May 7-11, 1995.
- [2] Moffat R.J., Danek C., "Final Report: The NIST/NSF Workshop on Heat Flux Transducer Calibration," at NIST in Gaithersburg, MD, January 23 and 24, 1995.
- [3] Grosshandler, W.L., Blackburn, D., "Development of a High Conduction Calibration Apparatus," HTD-Vol. 353, Proceedings of the ASME Heat Transfer Division, Vol. 3, pp.153-158, 1997.
- [4] Murthy, A.V., Tsai, B.K., Saunders, R.D., "Radiative Calibrations of Heat Flux Sensors at NIST-An Overview," HTD-Vol. 353, Proceedings of the ASME Heat Transfer Division, Vol. 3, pp.159-164, 1997.
- [5] Diller, T.E., "Advances in Heat Flux Measurements," Advances in Heat Transfer, v.23, Academic Press, Boston, 1993.
- [6] Diller, T. E., "Heat Flux," Ch. 6.3 In The Measurement, Instrumentation and Sensors Handbook, Ed. J. G. Webster, CRC Press, Boca Raton, Florida, 1998.
- [7] Keltner, N.R., "Heat Flux Measurements: Theory and Applications," Ch. 8, In K. Azar (ed.), Thermal Measurements in Electronics Cooling, Boca Raton: CRC Press, 273-320, 1997.
- [8] Holmberg, D., Steckler, K., Womeldorf, C., Grosshandler, W., "Facility for Calibrating Heat Flux Sensors in a Convective Environment," HTD-Vol. 353, Proceedings of the ASME Heat Transfer Division, V. 3, pp.165-171, 1997.
- [9] Personal communication with D. Blackburn of NIST Semiconductor Electronics Division.
- [10] Taylor, B.N., Kuyatt, C.E., "Guidelines for Evaluating and Expressing the Uncertainty of NIST Measurement Results," NIST Technical Note 1297, 1994.
- [11] Personal communication with R. Davis and E. Moore of NIST Chemical Science and Technology Laboratory.
- [12] Lemmon, E.W., "NIST Air Properties Database, SRD #72, Version 1.0," National Institute of Standards and Technology, Gaithersburg, MD, 1998.
- [13] Melling, A., et. al., "Interpolation Correlations for Fluid Properties of Humid Air in the Temperature Range 100°C to 200°C ," J. Physical Chemistry Ref. Data, Vol. 26, No. 4, 1997.